

Uranium adsorption studies on hydrothermal carbon produced by chitosan using statistical design method

Wen-Long Zhang · Zhi-Bin Zhang ·
Xiao-Hong Cao · Ru-Chao Ma · Yun-Hai Liu

Received: 28 November 2013 / Published online: 13 April 2014
© Akadémiai Kiadó, Budapest, Hungary 2014

Abstract A new hydrothermal cross-linking chitosan (HCC) was prepared by hydrothermal reaction at a mild temperature (180 °C) to diminish the solubility in acid solution, and the amine groups were almost retained during the hydrothermal reaction characterized by FT-IR and the dissolution rate in pH 3 solution decreased from 89.6 to 12.6 %. The effects of initial pH, contact time, initial concentration and temperature on the sorption capacity are discussed using 24 full-factorial central composite design using response-surface methodology. The HCC showed the highest uranium sorption capacity at initial pH of 7.92 and contact time of 273.6 min with 24 full-factorial central composite design and the maximum adsorption capacity was 273 mg/g. The adsorption process could be well defined by the Langmuir isotherm and the thermodynamic parameters, $\Delta G^\circ(298\text{ K})$, ΔH° and ΔS° , demonstrated shown that the sorption process of U(VI) onto HCC was feasible, spontaneous and endothermic in nature.

Keywords Chitosan · Hydrothermal carbonization · Adsorption · Uranium · Central composite design

Introduction

Adsorption, due to its high efficiency and ease of handling, has been developed for the removal and recovery of uranium from radioactive wastes in consideration of the dual significance of the potential environmental health threat and a nonrenewable resource of nuclear energy [1]. The carbonaceous materials such as activated carbon [2, 3], carbon nanotubes [4, 5] and carbon fiber [6] have been gradually applied to this area because of their higher thermal and radiation resistance than organic exchanger resins and better acid–base stability compared with familiar inorganic sorbents.

Chitosan, modified from chitin, is the second most abundant naturally polysaccharide in the world, which has good biological features such as non-toxicity, hydrophilicity, biocompatibility, biodegradability and antibacterial properties. On chitosan's chains, there are lots of free amine groups and hydroxyl groups, which have been reported to be coordination sites with metal ions [7]. Although chitosan has good adsorption capacity, it lacks good mechanical properties and it can be easily dissolved in acid solutions due to the presence of amine groups within its structure. Hence, numerous studies have been devoted to homogeneous or heterogeneous cross-linking of chitosan with di- or polyfunctional agents, such as sodium tripolyphosphate, glutaraldehyde, ethyleneglycol diglycidyl ether and epichlorohydrin [8–12]. However, the chemical crosslinking methods usually require many synthetic steps and in some toxic reagents are employed. Therefore it is necessary to investigate a “green” cross-linking method via a one-step process.

W.-L. Zhang · Z.-B. Zhang · X.-H. Cao · R.-C. Ma ·
Y.-H. Liu (✉)

Key Laboratory of Radioactive Geology and Exploration
Technology Fundamental Science for National Defense,
East China Institute of Technology, Nanchang 330013,
People's Republic of China
e-mail: walton_liu@163.com

W.-L. Zhang · Z.-B. Zhang · X.-H. Cao · R.-C. Ma · Y.-H. Liu
State Key Laboratory Breeding Base of Nuclear Resources and
Environment (East China Institute of Technology), Ministry of
Education, Nanchang 330013, People's Republic of China

W.-L. Zhang · Z.-B. Zhang · X.-H. Cao · R.-C. Ma · Y.-H. Liu
School of Chemistry, Biological and Materials Sciences,
East China Institute of Technology, Nanchang 330013,
People's Republic of China

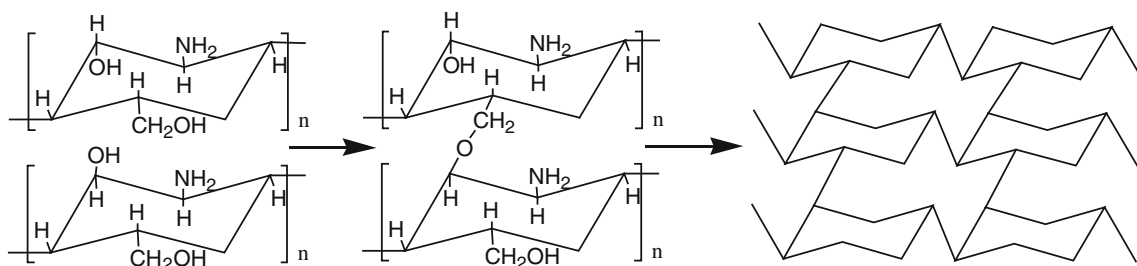


Fig. 1 A schematic illustration of the preparation procedure of HCC by hydrothermal carbonization of chitosan

The classical method of optimizing sorption conditions by varying the level of one parameter over a certain range, while holding the rest of the test variables constant. This single-factor-at-a-time strategy is generally time-consuming and requires a large number of experiments to be carried out. The effect of interactions between the variables isn't considered and the method is inadequate for a full understanding of the response surface.

In this work, a new hydrothermal cross-linking chitosan (HCC) was prepared by hydrothermal reaction at a mild temperature (180 °C). The synthetic procedure is illustrated in Fig. 1, its structural and compositional characteristics were determined by SEM and FT-IR. The effects of initial pH, contact time, initial concentration and temperature on the sorption capacity are discussed using 24 full-factorial central composite design employing response-surface methodology [13–15]. In addition, the adsorption kinetics, isotherm models and thermodynamics were also studied.

Materials and methods

Materials

Chitosan, with a deacetylation percentage of 85 % was purchased from the reagent factory of Shanghai of Chinese medicine crop. All the other chemical reagents were of AR grades. For the preparation of a stock uranium(VI) solution, 1.1,792 g U_3O_8 was put into a 100 mL beaker, and 10 mL hydrochloric acid ($\rho = 1.18$ g/mL), 2 mL 30 % hydrogen peroxide were added. The beaker was heated to evaporate the solution almost to dryness and then 10 mL hydrochloric acid was added into a solution. The solution was then transferred to a 1,000 mL volumetric flask, diluted with distilled water and shaken to produce the stock solution of 1 mg/mL uranium(VI). The uranium solutions were prepared by diluting the stock solution to appropriate volumes depending upon the experimental requirements.

Preparation of hydrothermal cross-linking chitosan

Typically, 2.0 g of pure chitosan (CTS) was dissolved in 18 mL 2 % (V/V) acetic acid solution and added into a

50 mL Teflon-lined stainless steel autoclave, and then sealed and tempered at 180 °C for 12 h. The products were finally filtered and washed with deionized water, and then dried.

Characterization

The zeta-potential value was obtained by POWEREACH JS94H micro-electrophoresis apparatus. Surface morphology was characterized on a JEOL JSM-5900 scanning electron microscopy. The FT-IR spectra were recorded on Nicolet Nexus 870 Fourier transform infrared spectrometer using the KBr pellet technique (1:50) with the resolution 2/cm. To determine the dissolution rate of CTS and HCC in aqueous solution, typically, 0.1 g sample was added to the aqueous solution with fixed initial pH varying from 3.0 to 10.0 adjusted by 0.1 mol/L NaOH and HCl solution and then shook for 12 h. The volume of solution was 100 mL and the dissolution temperature was 20 °C. This was followed by filtration and drying for 3 h at 50 °C. The dissolution rate was calculated by Eq. (1)

$$D = \frac{m_0 - m_e}{m_0} \times 100\%, \quad (1)$$

where m_0 is the initial mass of sample, and m_e is the mass of sample after dissolution.

Adsorption experiments

To determine the U(VI) adsorptive capacity onto samples, typically, 0.010 g of adsorbents was added to U(VI) solution with the fixed initial pH varying from 4.0 to 8.0 (adjusted with 0.1 mol/L HNO_3 and 0.1 mol/L NaOH) and with U(VI) concentrations ranging from 20 to 80 mg/L. The batch sorption was performed in a reciprocating water bath shaker with concussion speed of 200 rpm with predetermined time and intervals (60 min, 5 °C). The remaining U(VI) of solution was determined by the method of Arsenazo-III spectrophotometry by 721 spectrophotometer (Shanghai Spectrum Instruments Co., Ltd) [16]. The amounts of U(VI) adsorbed (q , mg/g) and distribution

coefficient (K_d , mg/L) were calculated according to the Eqs. (2) and (3)

$$q_e = \frac{(C_0 - C_e)V}{m}, \tag{2}$$

$$K_d = \frac{C_0 - C_e}{C_e} \times \frac{V}{m}, \tag{3}$$

where C_0 and C_e are the uranium concentration in the initial and equilibrium solution (mg/L) respectively; V the volume of the U(VI) solution(L), m is the mass of dry adsorbents (g).

Experimental design for adsorption studies

The optimum condition for sorption of UO_2^{2+} by HCC was determined by means of the central composite design (CCD) under response surface methodology (RSM). Statistical design of experiments refers to the process of planning to experiments so that appropriate data that can be analyzed by statistical methods will be collected resulting in valid and objective conclusions [17]. Response surface methodology is a collection of mathematical and statistical techniques based on the fit of a polynomial equation to the experimental data, which must describe the behavior of a data set with the objective of making statistical previsions [18]. The experiments were carried out by the four independent process variables, initial pH (X_1), temperature (X_2), initial UO_2^{2+} concentration (X_3) and contact time (X_4) chosen according to the central composite design (CCD). The optimization of UO_2^{2+} removal was performed using the four chosen independent process variables with seven replicates at centre points, employing a total of 31 experiments in this study. The design matrix for the four variables is varied at five levels (-2, -1, 0, +1, +2). The full model equation with linear and quadratic terms for predicting the optimal response was given as,

$$y_i = b_0 + \sum b_i X_i + \sum b_{ii} X_{ii}^2 + \sum b_{ij} X_i X_j. \tag{4}$$

In the equation, b_0 represents the intercept. The terms, b_i , b_{ii} , and b_{ij} represent the linear effects, second order effects, and dual interaction between the investigated parameters. For the current model investigated in this study, the second-order polynomial equation can be presented as,

$$Y = b_0 + b_1 X_1 + b_2 X_2 + b_3 X_3 + b_4 X_4 + b_{11} X_{21} + b_{22} X_{22} + b_{33} X_{23} + b_{44} X_{24} + b_{12} X_1 X_2 + b_{13} X_1 X_3 + b_{14} X_1 X_4 + b_{23} X_2 X_3 + b_{24} X_2 X_4 + b_{34} X_3 X_4. \tag{5}$$

The range and the level of experimental variables investigated in this study are shown in Table 1.

Table 1 Experimental independent variables

| Factor | Factor code | Levels and range (coded) | | | | |
|---|-------------|--------------------------|-----|-----|-----|-----|
| | | -2 | -1 | 0 | +1 | +2 |
| Initial pH | X_1 | 4 | 5 | 6 | 7 | 8 |
| Temperature (°C) | X_2 | 20 | 25 | 30 | 35 | 40 |
| Initial concentration (mg L ⁻¹) | X_3 | 20 | 35 | 50 | 65 | 80 |
| Contact time (min) | X_4 | 60 | 120 | 180 | 240 | 300 |

The four variables were varied at two levels (+1 and -1). The higher and the lower levels of the variables were designated as +1 and -1, respectively. The centre point was designated as 0, with -2 and +2 showing star points (a) which are calculated using the following equation:

$$\alpha = [\text{number of factorial points}]^{\frac{1}{4}}. \tag{6}$$

Codification of the variable levels consists of transforming each real value investigated into a coordinate on a scale with dimensionless values proportional to its localization in the experimental space [19].

The following equation can be used to transform a real value (z_i) into a coded value (x_i) for statistical calculations:

$$x_i = \frac{(z_i - z_i^0)}{\Delta z_i}, \tag{7}$$

where Δz_i is the difference between the real values designed for experiments and z_0 the real value at the central point. MatLab 7.1 and Excel were used for regression and graphical analysis of the data obtained. The optimum values of the selected variables were obtained by solving the regression equation and by analyzing the response surface contour plots.

Result and discussion

Characterization

FT-ir

The FT-IR spectra of pristine chitosan (CTS) and HCC are shown in Fig. 2. The broad band at 3,400/cm was assigned to the O-H and -NH₂ stretching vibration, and the peak appearing at 2,918 and 2,852/cm were due to the -CH₂ symmetric and asymmetric absorption, and the characteristic band at 1,661 and 1,419/cm was attributed to the C=O and C-N vibration in the amide group associated with few remaining acetamide groups present on the chain due to incomplete deacetylation of chitosan. The two peaks at 1,082 and 1,028/cm correspond to stretching vibrations of

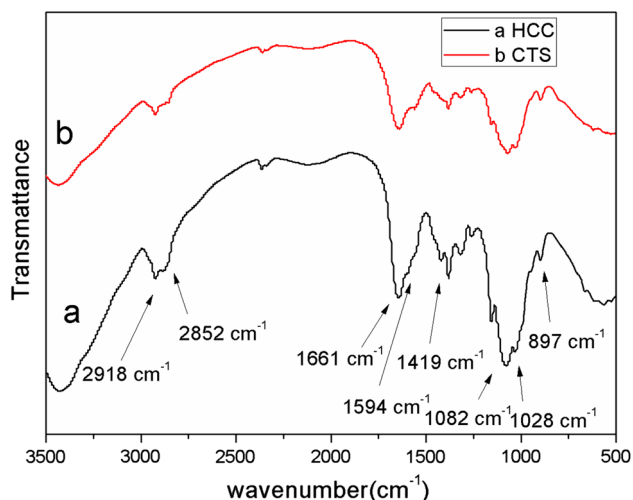


Fig. 2 FT-IR spectra of HCC (a) and CTS (b)

the primary and secondary $-OH$ groups respectively. The absorption band appearing at $900/cm$ was a characteristic absorption band of the beta-D-glucose unit. They all demonstrated that amine groups were almost retained during the hydrothermal reaction and HCC was rich in amino groups, which was also confirmed by that the zeta-potential value of HCC that was positive at the pH value below 6.5. These could be interpreted as the degradation of the chitosan chain and decomposition of the pyranose ring through dehydration. Amine groups didn't react with hydroxyl groups because its protonation in acid environment and hydroxy groups were not connected to strong electron-withdrawing group. Chitosan chain generate oligosaccharides and aromatic compounds in dehydration reaction; Oligosaccharides dehydration and intermolecular crosslinking in higher temperature.

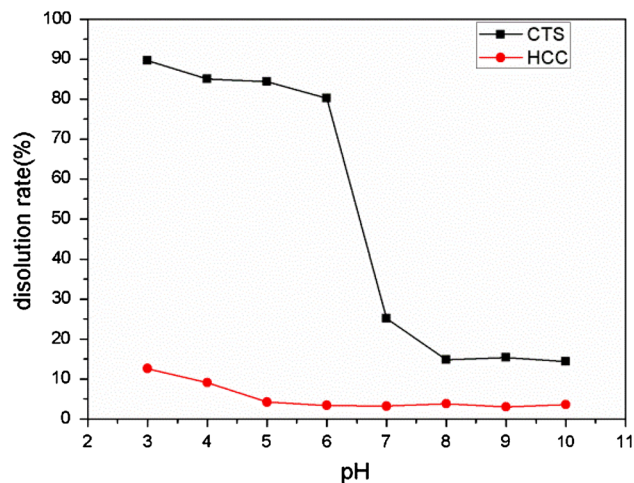


Fig. 4 The effect of pH on dissolution rate of CTS and HCC (temperature: $30\text{ }^{\circ}\text{C}$, contact time: 360 min)

SEM

Figure 3 showed the SEM images of HCC with magnification of 5,000 and 10,000, respectively. It could be seen that HCC has an irregular alveolate surface with some carbon microspheres ($2\text{ }\mu\text{m}$) and loose, porous structure. It demonstrated that hydrothermal carbonization for CTS was similar to hydrothermal carbon spheres (HCSs). However, amino groups tend not to be involved in hydrothermal reaction and cause irregular alveolate surface.

Dissolution rate

The dissolution rate of CTS and HCC are shown in Fig. 4. At lower pH, CTS can be easily dissolved due to its amine groups, dissolution rate reach up to 89.6 % at pH 3.0, then

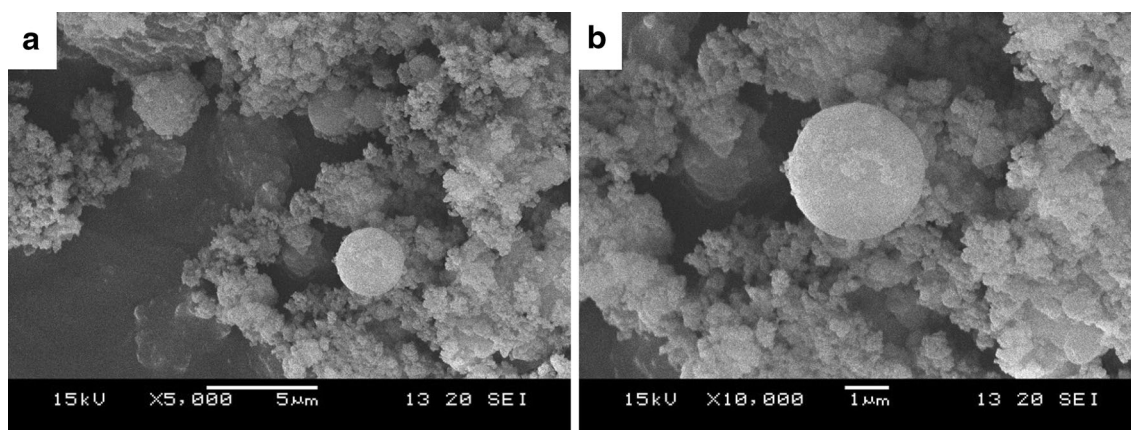


Fig. 3 The SEM image of different resolutions of HCC (a $\times 5,000$, b $\times 10,000$)

Table 2 ANOVA for the regression model for UO_2^{2+} uptake capacity of HCC

| Sources of variation | df | Sum of squares | Mean squares | F-value | Probability > F |
|----------------------|----|----------------|--------------|---------|-----------------|
| Regression | 14 | 35,923.8 | 2,566 | 32.66 | 0 |
| Residual | 16 | 1,257.2 | 78.60 | | |
| Total | 30 | 37,181.0 | | | |

$R^2 = 0.97$

keep this high rate till to pH 6.0. In contrast, HCC has degradation-resistance at low pH, dissolution rate was only 12.6 % at pH 3.0 and decreased to 4.2 % above pH 5.0. All these demonstrate that hydrothermal cross-linking was an effective way to prevent chitosan degradation in acidic medium.

The optimization of adsorption parameters

The effect of experimental variables such as the initial pH, the contact time, the initial concentration and the temperature on UO_2^{2+} adsorption capacity of the adsorbent were investigated using RSM according to the CCD. The experiments were carried out with 16 factorial points, nine star points (1 at the center) and six replicate points used in the central composite design.

The relationship between the independent variables and the responses are expressed by the following quadratic model:

$$\begin{aligned}
 Y = & 108 + 19.3X_1 + 7.6X_2 + 24X_3 \\
 & + 1.8X_4 - 14.9X_1^2 + 2.8X_2^2 + 4.7X_3^2 - 5.2X_4^2 \\
 & + 5.4X_1X_2 + 12X_1X_3 + 2.7X_1X_4 + 2.6X_2X_3 \\
 & + 1.5X_2X_4 + 3X_3X_4.
 \end{aligned}
 \tag{8}$$

The ANOVA (analysis of variance) of data was carried out at 96.6 % confidence level to check the fitting of the experimental values to the predicted ones (Table 2). *F* test for the significance level of data gave $P < 0.05$ with a model *F* value of 32.66 revealing that this regression is statistically significant. The correlation coefficient value (R^2) of 93.6 % indicated that there was a high correlation between the observed values and the predicted ones.

Significance of each coefficient present in Eq. (7) is determined by the student’s *t* test and *P*-values. The coefficients of independent variables *t* and *P* values according to the investigated parameters are given in Table 3. The influences of initial pH, temperature and initial concentration on the adsorption process were considered to be statistically significant as main affects ($P < 0.05$).

Table 3 Estimated regression coefficient and corresponding *t* and *P* values

| Regression | Coefficients | Standard error | <i>t</i> | <i>P</i> |
|------------|--------------|----------------|----------|----------|
| Intercept | 108.088 | 3.350 | 32.260 | 0.000 |
| X_1 | 19.314 | 1.809 | 10.674 | 0.000 |
| X_2 | 7.620 | 1.809 | 4.211 | 0.001 |
| X_3 | 24.015 | 1.809 | 13.273 | 0.000 |
| X_4 | 1.835 | 1.809 | 1.014 | 0.326 |
| X_1X_1 | -14.875 | 1.658 | -8.973 | 0.000 |
| X_2X_2 | 2.752 | 1.658 | 1.660 | 0.116 |
| X_3X_3 | 4.681 | 1.658 | 2.824 | 0.012 |
| X_4X_4 | -5.163 | 1.658 | -3.114 | 0.007 |
| X_1X_2 | 5.437 | 2.216 | 2.454 | 0.026 |
| X_1X_3 | 12.010 | 2.216 | 5.420 | 0.000 |
| X_1X_4 | 2.734 | 2.216 | 1.234 | 0.235 |
| X_2X_3 | 2.551 | 2.216 | 1.151 | 0.267 |
| X_2X_4 | 1.452 | 2.216 | 0.655 | 0.522 |
| X_3X_4 | 3.062 | 2.216 | 1.382 | 0.186 |

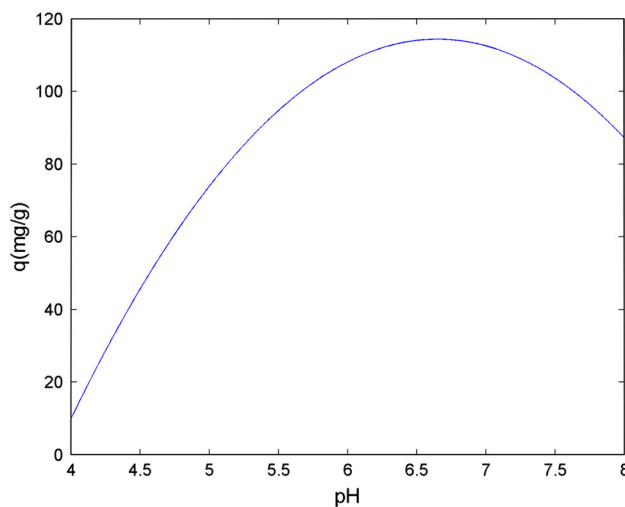


Fig. 5 pH effect on adsorption of UO_2^{2+} from aqueous solution by HCC (temperature: 30 °C, concentration: 50 mg/L, contact time: 180 min)

It is known that the larger the coefficient, the larger is the effect of the related parameter. When the effect of a factor is positive, an increase in the value of the removal efficiency is observed if the factor changes from low to high level. In contrast, if the effect is negative, a reduction in removal efficiency occurs for the high level of the same factor [20].

The positive values of coefficients related to the initial concentration ($X_3 = 24.015$) and temperature ($X_2 = 7.620$) indicate that the initial concentration and temperature have positive effects on the adsorption. However, initial pH

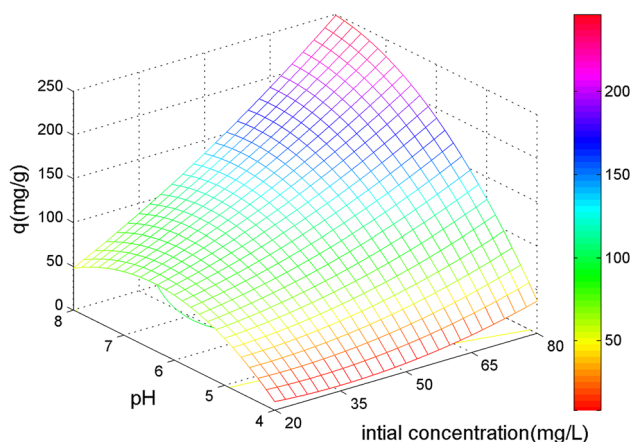


Fig. 6 Response surface plot for the effects of initial concentration and pH on adsorption of UO_2^{2+} from aqueous solution by HCC

coefficient ($X_1X_1 = -14.875$) has a negative cumulative effect on the adsorption of UO_2^{2+} from aqueous solution by HCC. Furthermore, the observation that the adsorption of UO_2^{2+} increases between pH 4.0–6.5 and decreases between pH 6.5–8.0 (Fig. 5) should also be taken account when considering the initial pH effect. The optimum experimental values in coded form were found for each parameter for the uptake capacity of UO_2^{2+} by Minitab: $X_1 = 1.96$, $X_2 = 2.00$, $X_3 = 2.00$, $X_4 = 1.56$.

These coded values can be transformed to real values using Eq. (6). The optimum values giving the maximum uptake of uranium ions (273 mg/g) were calculated to be at initial pH of 7.92, temperature of 40 °C, initial concentration of 80 mg/L and contact time of 273.6 min.

Effect of initial pH and initial concentration on the UO_2^{2+} uptake

Effluents from nuclear industry containing uranium have a variable pH (acidic to alkaline) [21]. The effects of initial pH and initial UO_2^{2+} concentration on the uptake are shown in Fig. 6. The metal uptake increased with increasing initial solution pH ranging from 4.0 to 6.5; pH values higher than 6.5 reduced the UO_2^{2+} uptake. On the other hand, metal uptake increased with increasing initial metal ions concentration ranging from 20 to 80 mg/L in all pH ranges.

The increase of metal uptake by increasing initial metal ions concentration is due to an increase in the driving force of the concentration gradient, rather than the increase in the initial metal ion concentration. Under the same conditions, if the concentration of metal ions in the solution is higher, the active sites of adsorbent are surrounded by more metal ions, and the process of adsorption is carried out more effectively. Therefore, the value of q increased with increasing initial metal ions concentration [22].

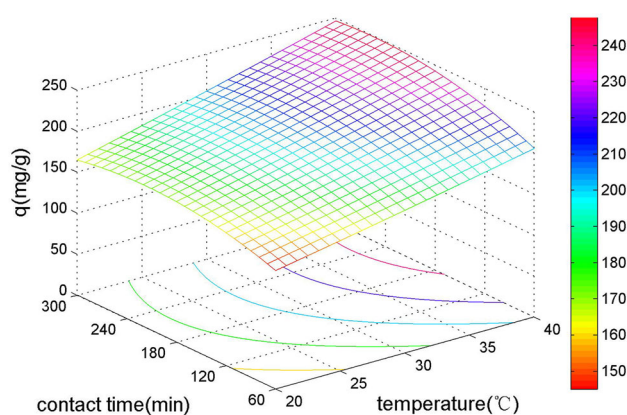


Fig. 7 Response surface plot for the effects of temperature and contact time on adsorption of UO_2^{2+} from aqueous solution by HCC

At lower pH conditions, UO_2^{2+} uptake was decreased due to increasing positive charge of the adsorbent surface. The pH values of aqueous solution influence the precipitation of U(VI) ions and ionization of surface functional groups. At low pH, the HCC surface was expected to be protonated and hence positively charged. Hence, adsorption of UO_2^{2+} ions was less preferred at low pH. An increase in pH resulted in a less positive HCC surface that adsorbed the cationic uranium species $[(\text{UO}_2)_2(\text{OH})_2^{2+}, \text{UO}_2\text{OH}^+, (\text{UO}_2)_3(\text{OH})_5^+]$. Around the circumneutral pH, U(VI) speciation was dominated by anionic uranyl carbonate $[(\text{UO}_2)_2\text{CO}_3(\text{OH})^{3-}, \text{UO}_2(\text{CO}_3)_3^{4-}, \text{UO}_2(\text{CO}_3)_2^{2-}]$ and hence adsorption onto HCC decreased beyond pH 7.0 [23].

Effect of contact time and temperature on the UO_2^{2+} uptake

The effect of contact time and temperature on the uptake of UO_2^{2+} is shown in Fig. 7. The U(VI) uptake increased with increasing temperature ranging from 20 to 40 °C, the adsorption capacity reinforced with the rise of temperature indicating that the process is endothermic. The U(VI) uptake by HCC increased sharply at the beginning, and then gradually reached equilibrium after 180 min, which was deemed sufficient to establish sorption equilibrium. The faster adsorption rate at the beginning would be due to the larger concentration gradient.

Confirmation experiments

Further to support the statistical approach which have applied is suitable for the experimental design used, the confirmatory experiments were conducted with the effects as suggested by the model (pH, initial concentration, contact time, temperature). The effect of pH, initial

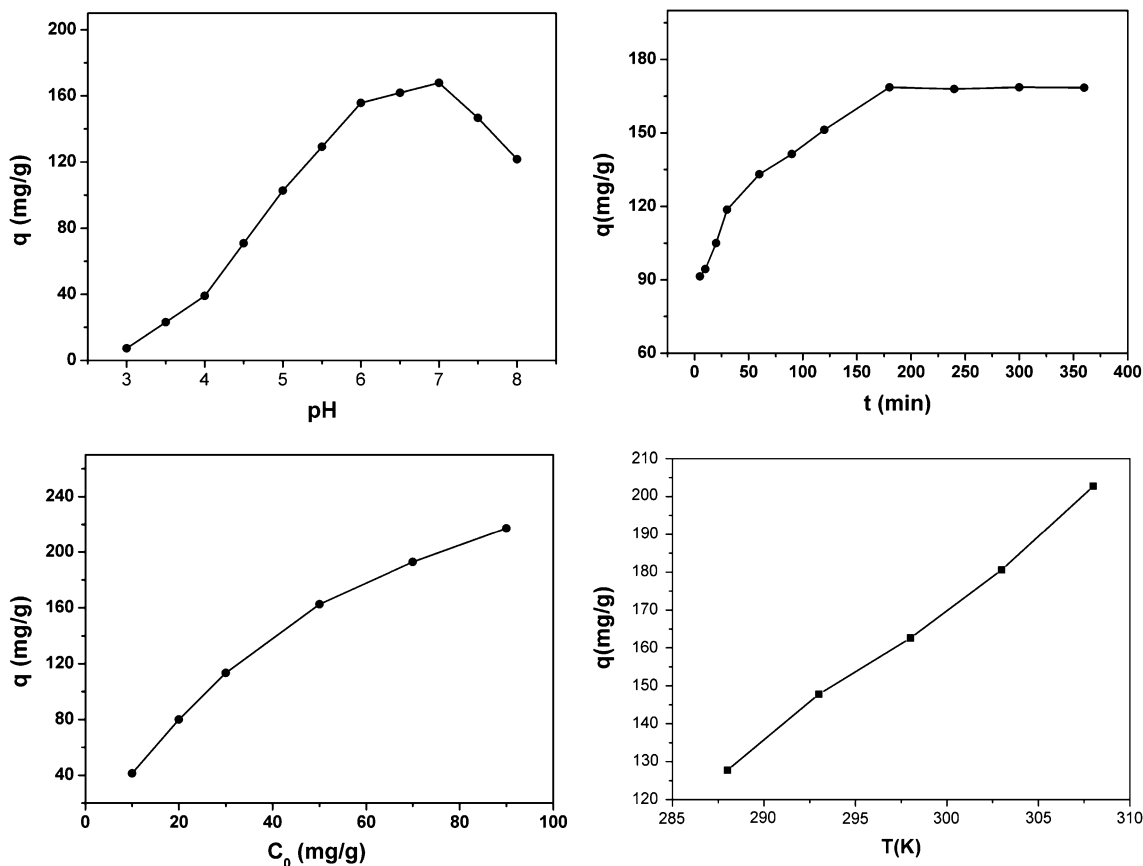


Fig. 8 Confirmation experiments of pH, contact time, initial concentration and temperature effect on adsorption of UO_2^{2+} from aqueous solution by HCC

concentration, contact time and temperature were shown in Fig. 8 and data is in accordance with the results obtained from optimized conditions.

Sorption kinetics studies

In order to explain the controlling mechanism of adsorption processes such as mass transfer and chemical reaction, two different kinetic models, pseudo-first order and pseudo-second order models were applied to test the sorption kinetics.

The pseudo-first order kinetic model and pseudo-second order kinetic model may be represented by Eqs. 9 and 10

$$\ln(q_e - q_t) = \ln q_e - k_1 t, \tag{9}$$

$$\frac{t}{q_t} = \frac{1}{k_2 q_e^2} + \frac{t}{q_e}, \tag{10}$$

where q_e and q_t refer to the amount of U(VI) adsorbed ($mg\ g^{-1}$) at equilibrium time and any time (min), respectively; k_1 (min^{-1}) and k_2 ($g\ mg^{-1}\ min^{-1}$) are the rate constant of first and second order adsorption.

The adsorption kinetic parameters in Eqs. 9 and 10 were calculated from the slopes and intercepts of the fitted curves, and the results were shown in Table 4. Obviously, the correlation coefficient, R^2 of the pseudo-second-order was better than pseudo-first-order, which indicated that the pseudo-second-order kinetic model was more suitable to describe the adsorption process of U(VI) onto HCC. Therefore, the adsorption process of U(VI) on HCC might be regarded as chemi-sorption, which could be the rate-controlling step.

Determination of thermodynamic parameters

To investigate the effect of temperature on the adsorption of uranium, thermodynamic parameters such as enthalpy (ΔH^0), entropy (ΔS^0) and Gibbs free energy (ΔG^0) must be taken into consideration in order to determine the spontaneity of a process. The adsorption thermodynamic parameters ΔH^0 , ΔS^0 and ΔG^0 could be calculated by the following Eqs. (11), (12) and (13) [24, 25]

$$\Delta G^0 = -RT \ln K_D, \tag{11}$$

Table 4 Kinetic parameters for adsorption of U(VI) onto HCC

| Adsorbents | Pseudo-first-order kinetics | | | Pseudo-second-order kinetics | | |
|------------|-----------------------------------|----------------------------|--------|-----------------------------------|--|--------|
| | $q_{1,cal}$ (mg·g ⁻¹) | k_1 (min ⁻¹) | R^2 | $q_{2,cal}$ (mg·g ⁻¹) | k_2 (g·mg ⁻¹ ·min ⁻¹) | R^2 |
| HCC | 72.59 | 0.02 | 0.8622 | 170.13 | 4.39×10^{-4} | 0.9967 |

Table 5 The thermodynamic parameters for UO₂²⁺ adsorption on HCC

| Adsorbents | ΔH (kJ/mol) | ΔS (J mol ⁻¹ K ⁻¹) | ΔG (kJ/mol) | | |
|------------|---------------------|---|---------------------|------------|------------|
| | | | 288.15 (K) | 298.15 (K) | 308.15 (K) |
| HCC | 23.53 | 165.13 | -24.06 | -25.71 | -27.36 |

Table 6 Comparison of the thermodynamic parameters and optimal uranium sorption capacity with previous related studies

| Adsorbents | Thermodynamic parameters | | Optimal UO ₂ ²⁺ sorption capacity (mg/g) | Reference |
|---------------------|--------------------------|----------------------------|--|-----------|
| | ΔH (kJ/mol) | ΔG (298 K, kJ/mol) | | |
| HCC | 23.53 | -25.71 | 273.0 | |
| HTC | 36.10 | -14.40 | 62.7 | [27] |
| HTC-COOH | 27.50 | -21.80 | 205.8 | [27] |
| HCS | 12.44 | -17.92 | 57.4 | [28] |
| HCS-PO ₄ | 11.20 | -22.28 | 157.0 | [28] |
| CMK-3 | 21.52 | -7.71 | 178.6 | [26] |
| CMK-3-COOH | 8.21 | -10.45 | 250.0 | [26] |

$$\ln K_D = \frac{\Delta S^0}{R} - \frac{\Delta H^0}{RT}, \quad (12)$$

$$\Delta G^0 = \Delta H^0 - T\Delta S^0. \quad (13)$$

where K_D is the Langmuir constant, ΔS^0 is the change of entropy (J mol⁻¹ K⁻¹), ΔH^0 is the change of enthalpy (kJ/mol), T is the absolute temperature in Kelvin (K) and R is the gas constant (8.314 J mol⁻¹ K⁻¹). ΔH^0 and ΔS^0 can be calculated from the slope and intercept of the straight line (Fig. 8). The change of Gibbs free energy values are calculated from Eq. 10.

The results were shown in the Table 5. The positive value of enthalpy change ΔH^0 indicated that the sorption process was endothermic. The negative values of ΔG^0 indicated that the adsorptive performance of UO₂²⁺ on the HCC was feasible and spontaneous. Moreover, the decrease of ΔG^0 values with temperature increasing shows that the adsorption process was more favorable at higher temperature, the positive value of ΔS^0 showed the randomness at the solid-solution interface was increasing during the adsorption process [26]. Comparison of the thermodynamic parameters and optimal uranium sorption

capacity with previous related studies was shown in Table 6.

Adsorption isotherm

The adsorption isotherms indicate how the adsorption molecules distribute between the liquid phase and the solid phase when the adsorption process reaches equilibrium state [29]. In order to deeply study the sorption process of the adsorbents, the equilibrium data have been subjected different sorption isotherms, namely Langmuir [30], Freundlich [31] models. The Langmuir equation can be described by the linearized Eq. 14 [32]

$$\frac{C_e}{q_e} = \frac{1}{K_L q_m} + \frac{C_e}{q_m}, \quad (14)$$

where C_e is the equilibrium concentration (mg/L), q_e is the amount of solute sorbed per unit weight of sorbent (mg/g), q_m is the Langmuir constant, which represents the saturated monolayer sorption capacity (mg/g). K_L is a constant related to the energy of adsorption.

The Freundlich model can be applied to nonideal sorption on heterogeneous surfaces as well as multilayer sorption [33]. The empirical Freundlich equation can also be transformed into linearized Eq. 15

$$\ln q_e = \ln K_F + \frac{1}{n} \ln C_e, \quad (15)$$

where C_e is the equilibrium concentration (mg/L), q_e is the amount of solute sorbed per unit weight of sorbent (mg/g), K_F is the Freundlich constant related to the adsorption capacity, and n is relevant to the adsorption intensity.

The adsorption constants evaluated from the isotherms with the correlation coefficients (R^2) were given in Table 7 Langmuir isotherm was found to be more suitable to describe the sorption characteristics of U(VI) on HCC when comparing the values of correlation coefficients of both models. The result indicated that the present adsorption process on HCC probably dominated by a monolayer adsorption rather than a multilayer one.

Table 7 Parameters of Langmuir and Freundlich isotherm for UO_2^{2+} adsorption on HCC

| Adsorbents | Langmuir isotherm | | | Freundlich isotherm | | |
|------------|-------------------|--------------------|--------|---------------------|------|--------|
| | K_L | $q_m(\text{mg/g})$ | R^2 | K_F | n | R^2 |
| HCC | 0.10 | 264.55 | 0.9967 | 39.56 | 0.45 | 0.9543 |

Conclusion

In the present work, a new HCC was prepared by hydrothermal reaction at a mild temperature (180 °C) to diminish the solubility in acid solution, and the amine groups were almost retained during the hydrothermal reaction characterized by FT-IR and the dissolution rate in pH 3.0 solution decreased from 89.6 to 12.6 %. The effects of initial pH, contact time, initial concentration and temperature on the sorption capacity are discussed using 24 full-factorial central composite design using response-surface methodology.

The uranium uptake experiments using 24 full-factorial central composite design showed 96 % confidence level. The F test gave $P < 0.05$ with a model F value of 32.66 which revealed that this regression is statistically significant. The correlation coefficient value (R^2) of 93.6 % indicated that there was a high correlation between the observed values and the predicted ones. The HCC showed the highest uranium sorption capacity at initial pH of 7.92 and contact time of 273.6 min with 24 full-factorial central composite design and the maximum adsorption capacity was 273 mg/g. The adsorption process could be well defined by the Langmuir isotherm and sorption process of U(VI) onto HCC was feasible, spontaneous and endothermic in nature.

Acknowledgments We gratefully acknowledge the financial support provided by National Natural Science Foundation of China (Grant Nos. 21101024, 21201033, 21301028), National Undergraduate Training Programs for Innovation and Entrepreneurship (201210405006), Key Project of Chinese Ministry of Education (Grant No. 211086), the Young Scientists Training Program of Jiangxi Province (Grant No. 20122BCB23023), Natural Science Foundation of Jiangxi Province (Grant Nos. 20114BAB203002, 20122BAB203012, 20132BAB203027), China Postdoctoral Science Foundation (Grant No. 20110490857), and Project of Jiangxi Provincial Department of Education (Grant Nos. GJJ13452).

References

- Rao TP, Metilda P, Gladis JM (2006) *Talanta* 68:1047–1064
- Coleman SJ, Coronado PR, Maxwell RS, Reynold JG (2003) *Environ Sci Technol* 37:2286–2290
- Zhao YS, Liu CX, Feng M, Chen Z, Li SQ, Tian G, Wang L, Huang JB, Li SJ (2010) *J Hazard Mater* 176:119–124
- Schierz A, Zanker H (2009) *Environ Pollut* 157:1088–1094
- Shao DD, Jiang ZQ, Wang XK, Li JX, Meng YD (2009) 113: 860–864
- Xu Y, Zondlo JW, Finklea HO, Brennsteiner A (2000) *Fuel Process Technol* 68:189–208
- Wan Ngah WS, Fatinathan S (2008) *Chem Eng J* 143:62
- Crini G (2005) Recent developments in polysaccharide-based materials used as adsorbents in wastewater treatment. *Prog Polym Sci* 30:38–70
- Guibal E (2004) Interactions of metal ions with chitosan-based sorbents: a review. *Sep Purif Technol* 38:43–74
- Chen AH, Liu SC, Chen CY et al (2008) Comparative adsorption of Cu (II), Zn (II), and Pb(II) ions in aqueous solution on the crosslinked chitosan with epichlorohydrin. *J Hazard Mater* 154(1):184–191
- Akkaya R, Ulusoy U (2008) Adsorptive features of chitosan entrapped in polyacrylamide hydrogel for Pb^{2+} , UO_2^{2+} , and Th^{4+} . *J Hazard Mater* 151:380–388
- Wang G, Liu J, Wang X, Xie Z, Deng N (2009) Adsorption of uranium (VI) from aqueous solution onto cross-linked chitosan. *J Hazard Mater* 168:1053–1058
- Cochran WG, Cox GM (1957) *Experimental designs*
- Khuri AI, Cornell JA (1987) *Response surface: design and analysis*. Marcell Decker Inc., New York
- Montgomery DC (1991) *Design and analysis of experiments*, 3rd edn. Wiley, New York
- Nie B, Zhang Z, Cao X et al (2013) Sorption study of uranium from aqueous solution on ordered mesoporous carbon CMK-3. *J Radioanal Nucl Chem* 295(1):663–670
- Montgomery DC (1996) *Design and analysis of experiments*, 4th edn. John Wiley & Sons, New York
- Bezerra MA, Santelli RE, Oliveira PE, Villar LS, Escaleira LA (2008) *Talanta* 76:965–977
- Cana MY, Yildiz E (2006) *J Hazard Mater* B135:165–170
- Carmona MER, da Silva MAP, Leite SGF (2005) *Process Biochem* 40:779–788
- Bhat SV, Melo JS, Chaugule BB, D'Souza SF (2008) Biosorption characteristics of uranium(VI) from aqueous medium onto *Catenella repens*, a red alga. *J Hazard Mater* 158:628–635
- Ghorbania F, Younesia H, Ghasempouria SM, Zinatizadeh AA, Aminia M, Daneshia A (2008) *Chem Eng J* 145:267–275
- Kumar S, Loganathan VA, Gupta RB et al (2011) An assessment of U (VI) removal from groundwater using biochar produced from hydrothermal carbonization. *J Environ Manag* 92(10):2504–2512
- Ho YS, Ofomaja AE (2005) *Process Biochem* 40:3455
- Malkoc E, Nuhoglu Y (2005) *J Hazard Mater* 127:120
- Wang YQ, Zhang ZB, Liu YH et al (2012) Adsorption of U (VI) from aqueous solution by the carboxyl-mesoporous carbon. *Chem Eng J* 198:246–253
- Liu YH, Wang YQ, Zhang ZB et al (2013) Removal of uranium from aqueous solution by a low cost and high-efficient adsorbent. *Appl Surf Sci* 273:68–74
- Zhang Z, Zhou Z, Cao X et al (2014) Removal of uranium (VI) from aqueous solutions by new phosphorus-containing carbon spheres synthesized via one-step hydrothermal carbonization of glucose in the presence of phosphoric acid. *J Radioanal Nucl Chem* 299(3):1479–1487
- Hameed BH, Din ATM, Ahmad AL (2007) *J Hazard Mater* 141:819–825
- Langmuir I (1918) *J Am Chem Soc* 38:1361–1403
- Freundlich H (1906) *J Phys Chem* 57(1906):385–470
- Hazer O, Kartal S (2010) *Talanta* 82:1974–1979
- Parab H, Joshi S, Shenoy N, Verma R, Lali A, Sudersanan M (2005) *Bioresour Technol* 96:1241–1248